

A New Framework for Assessment of Potassium-Buffering Mechanisms

A. R. GARDNER-MEDWIN

*Department of Physiology
University College London
London WC1E 6BT, England*

Much information is now available about the dynamics of extracellular diffusion and the role of glial cells in potassium (K^+) homeostasis in a few tissues. Assessment is made complicated, however, by differences in geometry and the types of disturbance to which tissues are subject, while different buffer mechanisms work more effectively in different circumstances. This paper sets out a new framework for assessment of buffer mechanisms, based on a concept of "buffer capacity." This concept is applied to the K^+ homeostasis of both brain and retinal tissue.

THE CONCEPT OF "BUFFER CAPACITY" AS AN EQUIVALENT DISTRIBUTION VOLUME

A mechanism that buffers the extracellular K^+ concentration (K_o) is, by definition, one that reduces the K_o changes due to a disturbance. The percentage reduction that results from any one mechanism depends, in general, on the other mechanisms that are simultaneously operating; therefore the reduction does not, itself, form the basis for a satisfactory measure of buffer effectiveness that can be handled easily and combined for different mechanisms.

The concept of buffer capacity is based on that of an equivalent K^+ distribution volume. The simplest component of the distribution volume for K^+ released from neurons is, of course, the extracellular space. Buffer capacity is expressed in the same units as extracellular space (liters per liter of tissue) and is defined, subject to constraints discussed below, as the additional extracellular space that would have the same effect as a buffer mechanism.

FIGURE 1 shows the relation between the extracellular space in a small region of tissue and the various fluxes into and out of it. The K^+ concentration (K_o) is expressed in terms of a displacement (c) from a baseline level (c_b). The disturbance is caused by a flux, q , which is positive during K^+ release and negative during the subsequent reuptake of K^+ into the neurons that have undergone release. The buffer mechanisms account for fluxes f_j , not necessarily with the same time course as q , that normally diminish the effects of q . By direct accounting for all the K^+ movements, assuming a fixed extracellular space fraction α , we obtain an equation relating the rate of change of c (dc/dt) to the fluxes:

$$q = \alpha \, dc/dt + \Sigma f_j \tag{1}$$

where Σ indicates summation of the various buffer fluxes. The buffer capacity ϕ_j corresponding to each of the fluxes, f_j can now be defined formally as:

$$\phi_j = f_j / (dc/dt) \tag{2}$$

This definition, with substitution in Equation 1, gives a relationship expressing the equivalence between buffer capacities and additional extracellular space:

$$dc/dt = q / (\alpha + \Sigma \phi_j) \tag{3}$$

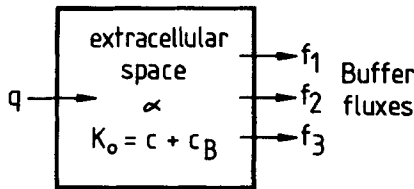


FIGURE 1. Influences on the extracellular K^+ concentration (K_o). The box represents extracellular space (volume fraction α) within a small region of tissue. A disturbance flux (q) alters K_o by an amount c from its baseline level c_B . Buffer fluxes f_j , and so forth, diminish the effects of q . The fluxes q, f are per unit tissue volume. K_o, c, c_B are local concentrations within extracellular space.

Assessment of a buffer mechanism in terms of its buffer capacity has the following merits that are evident from Equation 3:

1. There is a simple relation between flux, buffer capacity, and concentration changes.
2. It is possible to add buffer capacities for different mechanisms to obtain the total effective buffer capacity.

The extracellular space can itself be regarded as a primary buffer, with a capacity ϕ_{ec} equal to its volume fraction α , about 0.2 for superficial cortical tissue in the rat.¹ This provides a baseline for comparison of buffer capacities. Only mechanisms with buffer capacities comparable to, or greater than, the extracellular volume fraction can be regarded as physiologically significant. A total buffer capacity of 1.0 ($\alpha + \Sigma \phi_j$ in Eq. 3) would achieve an 80% reduction of K_o changes compared with distribution in extracellular space alone.

BUFFER CAPACITIES WITH FLUCTUATING DISTURBANCES

If a K^+ disturbance is fluctuating in time, the individual buffer fluxes may not all have the same time course. Consider the case of buffering by a tissue compartment that is always in complete equilibrium with extracellular space. For this, f_j into the compartment will always reflect the rate of change of K_o and be exactly proportional to it. From Equation 2, ϕ_j will be a simple constant, equal to the distribution volume of the compartment. Fluxes due to other mechanisms usually lag, to varying extents, behind (dc/dt) , and ϕ_j is not a simple constant.

The standard approach to such problems is to consider first of all pure sinusoidal disturbances, which are relatively simple. General disturbances can be analyzed into a combination of pure sinusoidal (Fourier) components, each with a characteristic frequency γ . The buffering of these components can be assessed independently and the resultant concentration changes added together. The special thing about sinusoidal disturbances is that, provided the effects of different disturbances add linearly, all the time-varying parameters of the system (such as the buffer fluxes) are sinusoidal also, at the same frequency. Not all physiological buffer mechanisms are linear.² For small disturbances they are approximately linear, however, while even for large disturbances many of the important features emerge from a quasi-linear analysis.²

For a sinusoidal K^+ disturbance, the buffer flux f_j is characterized by two parameters, peak amplitude and time lag relative to dc/dt (FIG. 2A). The lag is conveniently expressed as an angle called the phase lag θ ($=360^\circ \times \text{time lag/period}$). Buffer capacities can then be treated as vectors (i.e., arrows on a page), with a length equal to the ratio peak flux:peak dc/dt (Eq. 2) and with direction determined by the phase lag θ (FIG. 2B). Addition of buffer capacities is then equivalent to the addition of vectors (FIG. 2C) to give a resultant (ϕ_{tot}) whose length determines the magnitude of concentration changes (just as if it were a simple distribution space), and whose direction determines the phase of the concentration changes (i.e., when they occur relative to the disturbance).

Equations for vector quantities are expressed, for completeness and conciseness, in complex number notation ($i^2 = -1$). It is not necessary to understand this notation to appreciate the principal conclusions.

TIME COURSE AND FREQUENCY COMPONENTS OF TYPICAL NEURONAL DISTURBANCES

We need to consider the frequency components for typical neuronal disturbances in order to establish the frequency ranges for which buffering is likely to be important. Release of K^+ from neurons is rapid (over msec) when there are action potentials or synaptic potentials. The subsequent reuptake (q negative: FIG. 3A) is relatively slow, governed largely by the raised intracellular sodium concentration and the dynamics of the Na-K pump. Reuptake may be stimulated also by raised K_o , but note that for much of the reuptake period K_o is usually around or below normal.²

The time constant for reuptake of K^+ into neurons (τ_{reuptake}) has not been directly measured but is probably 20 seconds or more in mammalian brain tissue.² In the absence of buffering, the resulting disturbance of K_o would follow the time integral

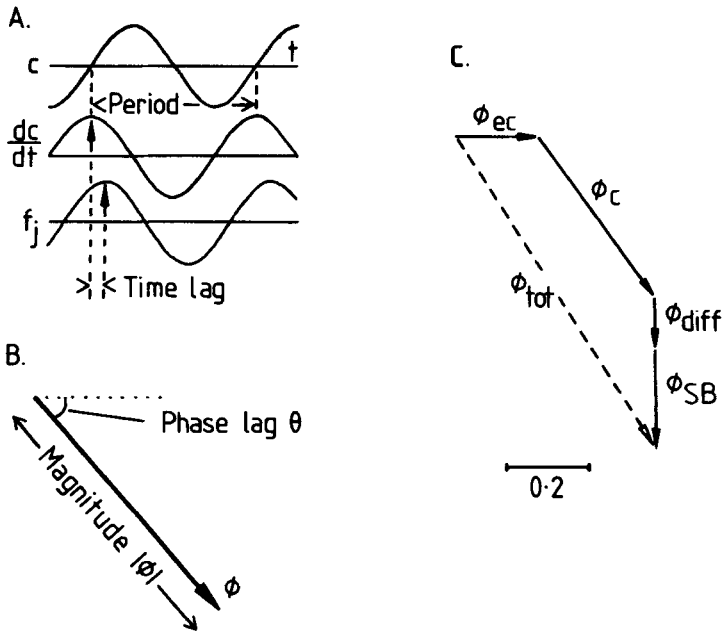


FIGURE 2. Buffer capacities for sinusoidal disturbances. (A) All parameters vary sinusoidally, but the buffer flux may lag relative to dc/dt . (B) The buffer capacity ϕ is a vector with magnitude $|\phi|$ equal to the ratio of the peak values of f_j and dc/dt . The phase lag $\theta = 360^\circ \times \text{time lag}/\text{period}$. (C) Total buffer capacity is the sum of capacity vectors due to separate buffer mechanisms, in this case extracellular space ($\phi_{ec} = \alpha$), cytoplasmic uptake (ϕ_c ; Eq. 4), diffusion (ϕ_{diff} ; Eq. 7) and spatial buffer action (ϕ_{SB} ; Eq. 9), all for a disturbance at 0.01 Hz with a wavelength of 1 mm. The major contribution to the overall buffer capacity (ϕ_{tot}) under these conditions is due to ϕ_c , with ϕ_{diff} relatively insignificant.

of q (FIG. 3B), rising sharply and declining with the time constant $\tau_{reuptake}$. The Fourier power spectrum for the components of this disturbance (FIG. 3C) gives the frequencies for which buffering can significantly diminish fluctuations of K_o due to neuronal release, even when the overall release pattern is a superposition of patterns such as FIG. 3A at random times due to asynchronous firing. A characteristic frequency $\Gamma = (2\pi\tau_{reuptake})^{-1}$, about 0.01 Hz for $\tau_{reuptake} = 20$ sec) divides the area under this curve into two equal portions. If a buffer mechanism has a significant buffer capacity only for frequencies much higher or much lower than Γ , then it leaves most of the spectrum unaffected.

BUFFERING DUE TO CYTOPLASMIC UPTAKE

Net uptake of K^+ into cytoplasm of neurons and glia in response to an increase of K_o , by passive and/or active means,^{3,4} represents a buffer mechanism that operates

even for uniform disturbances when there are no dispersal gradients. Data from the rat cerebral cortex^{5,6} indicates that a release of approximately 1.0 mmol K^+ per liter of tissue is required to produce a 1 mM increase of K_o . Since a capacity of approximately 0.2 (liter per liter of tissue) is extracellular, approximately 0.8 must be due to cytoplasmic uptake. This cytoplasmic capacity, designated v (≈ 0.8), is approximately equal to the cytoplasmic volume, corresponding to the fact that cells tend to increase their cytoplasmic K^+ concentration by about the same absolute amount as a change of extracellular concentration.

If we assume that cytoplasmic equilibration is linear with a simple exponential time constant τ_{eq} (for a sudden, maintained K_o alteration²), then we can derive the buffer capacity vectors for sinusoidal disturbances with any given frequency γ (FIG. 4). For low frequencies the capacity vector becomes more horizontal (equivalent to a simple distribution space) and larger, approaching 0.8 at zero frequency. Taking τ_{eq} as 22 seconds (probably a high estimate for cells in the central nervous system⁷), the total resultant buffer capacity (cytoplasmic and extracellular) at the characteristic frequency Γ for neuronal events (0.01 Hz: see above), is 0.60 (FIG. 4), compared with 0.2 for extracellular space alone. A general equation for the cytoplasmic buffer capacity ϕ_o can be derived:

$$\phi_o = v (1 + 4\pi^2 \tau_{eq}^2 \gamma^2)^{-1} (1 - 2\pi i \tau_{eq} \gamma) \quad (4)$$

BUFFERING BY EXTRACELLULAR DIFFUSION WITHIN EXTENSIVE TISSUE

Buffering by extracellular diffusion and by spatial buffering (see next section) occur only when disturbances are nonuniform throughout the tissue or when a tissue bound-

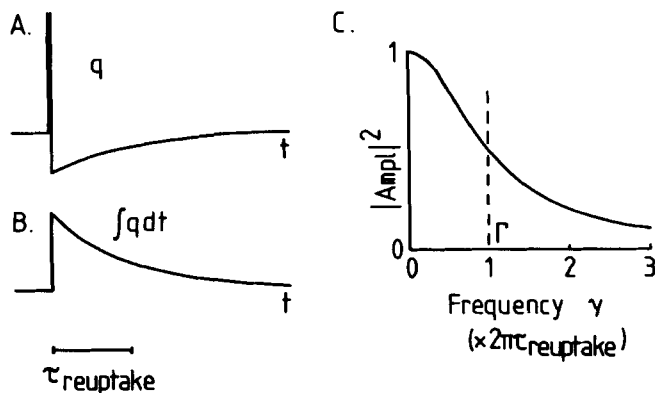


FIGURE 3. Disturbance associated with neuronal release and reuptake. (A) Time course of net K^+ release (q) due to a single brief neural event. (B) Time integral of q , proportional to the disturbance of K_o if there is no buffering. (C) Squared amplitude of the sinusoidal Fourier components of B: $(1 + 4\pi^2 \gamma^2 \tau^2)^{-1}$. Γ (ca. 0.01 Hz) is a characteristic frequency that divides the power spectrum (C) into two equal areas.

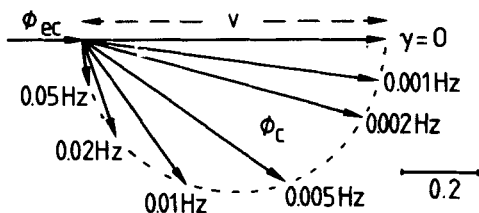


FIGURE 4. Buffering capacities associated with cytoplasmic uptake. Vectors (ϕ_c) for different frequency components of a disturbance are given for $\tau_{eq} = 22$ sec and $v = 0.8$ (Eq. 4). Extracellular capacity $\phi_{ec} = 0.2$ is shown for comparison.

ary is nearby. This section deals with nonuniform disturbances in tissue that is extensive and has homogeneous buffering properties.

A nonuniform disturbance can be analyzed into components that have pure sinusoidal variations in both space and time. The space dependence is characterized by wavelengths (W_k) in three perpendicular directions x_k (for $k = 1,2,3$). Extracellular diffusion flux f_k in the direction x_k is given³ by:

$$f_k = - \alpha D \lambda^{-2} \partial c / \partial x_k \tag{5}$$

where α is the extracellular volume fraction, D the K^+ diffusion coefficient, and λ the tortuosity factor, assumed equal in all directions.³ The diffusion flux differs from other buffer fluxes in that it neither enters nor leaves the extracellular space. It nevertheless represents dispersal from any one region of extracellular space and can be included as a buffer flux in FIGURE 1. The dispersal flux attributable to diffusion (f_{diff}) is obtained by differentiation of Equation 5. For a disturbance that is sinusoidal with wavelength W in one dimension it is:

$$f_{diff} = 4\pi^2 \alpha D \lambda^{-2} W^{-2} c \tag{6}$$

This flux is always in phase with c , which means that the buffer capacity is a vertical vector (phase lag 90° : FIG. 2). The corresponding buffer capacity, ϕ_{diff} , for a wavelength W and frequency γ is illustrated in FIGURE 5 (solid lines).

$$\phi_{diff} = - 2\pi i D \gamma^{-1} \alpha \lambda^{-2} W^{-2} \tag{7}$$

For disturbances with sinusoidal components in three dimensions, W^{-2} in Equations 6 and 7 becomes $\Sigma_j (W_j^{-2})$.

The buffer capacity due to diffusion falls for high frequency and long-wavelength disturbances (FIG. 4). At the characteristic frequency Γ for neural events (ca. 0.01 Hz), the capacity is greater than 0.5 for wavelengths less than 0.5 mm (FIG. 5). A local patch of active cells less than about 0.25 mm across (in three dimensions) would accordingly produce a K^+ disturbance that is buffered principally by diffusion. For much larger patches, diffusion becomes a relatively unimportant buffer, except for very slow components of a disturbance.

SPATIAL BUFFERING BY GLIAL CELLS WITHIN EXTENSIVE TISSUE

Spatial buffer action is the dispersal of extracellular K^+ by current flow through glial cells.⁷ The buffer flux (FIG. 1) is in this case flux carried from extracellular space into glial cells by glial membrane current (less a small fraction, about 1.2%, due to current in extracellular space). Since this flux occurs only when there are gradients of K_o in the tissue, under the same conditions as extracellular diffusion flux, it simplifies the mathematical expressions to express the buffer capacity due to spatial buffer action in terms of its ratio to the diffusion capacity ϕ_{diff} , already given in Equation 7. There are two important tissue parameters in relation to spatial buffering. In an earlier treatment of the topic² these were termed Λ (the electrotonic space constant for the glial network) and β (the ratio of spatial buffer flux to diffusion flux for long-wavelength disturbances). β is related to the cytoplasmic and extracellular resistances, r_i and r_o , respectively, and to the extracellular transport number³ for K^+ (n_K : ca. 0.012) by the equation:

$$\beta = (n_K^{-1} - 1)r_o(r_i + r_o)^{-1} \tag{8}$$

The buffer capacity ϕ_{SB} defined by Equation 2 is (from Eqs. 15, 16, 22, and 32 of the previous analysis²):

$$\phi_{SB} = \beta (1 + 4\pi^2 \Lambda^2 W^{-2})^{-1} \phi_{diff} \tag{9}$$

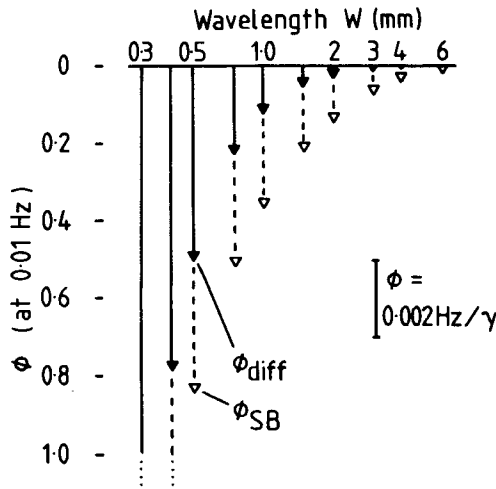


FIGURE 5. Buffer capacity vectors for diffusion (ϕ_{diff} : solid lines) and spatial buffering (ϕ_{SB} : broken lines). Phase lag in all cases is 90° . Scale at left is for 0.01 Hz, at right for general frequencies (γ). W is the effective wavelength; for disturbances in two or three dimensions, $W = (\Sigma W_j^{-2})^{-0.5}$. $\Lambda = 0.2$ mm, $\beta = 5$ for ϕ_{SB} (Eq. 9).

The ratio ϕ_{SB}/ϕ_{diff} approaches β (ca. 5.0 for rat cortex) for long-wavelength disturbances. Spatial buffer capacities for the parameters β , Λ for rat cortex^{5,6} are shown in FIGURE 5 (dashed lines), where they are added to the diffusion capacities (solid). At 0.01 Hz (Γ), ϕ_{SB} boosts the total buffer capacity for dispersal processes mainly for wavelengths around 0.5-1 mm, roughly the range where ϕ_{diff} is itself becoming insignificant. At a wavelength of 0.75 mm, the dispersal capacity is increased from 0.22 (diffusion alone) to 0.51 (diffusion + spatial buffer). For frequencies less than 0.01 Hz, the spatial buffer effects are larger and extend to longer wavelengths. For example, at 0.002 Hz and $W = 1.5$ mm, the combined capacity is 1.1, compared to 0.28 with diffusion alone.

The space constant for spatial buffering is substantially shorter in the frog tectum ($\Lambda = 0.05$ mm^{8,9}) than in the rat cortex (0.2 mm). This means that the benefit of spatial buffer action extends to higher frequencies and shorter wavelengths. For example at 0.01 Hz and $W = 0.75$ mm, $\phi_{diff} + \phi_{SB}$ becomes 1.2 (cf. 0.51 with $\Lambda = 0.2$ mm).

CHANGES OF EXTRACELLULAR VOLUME

At least two mechanisms result in decreases of the extracellular space fraction when there is raised K_o . In both cases the fluid movement out of extracellular space arises because there is a net loss of extracellular osmotic particles, in the first case because of KCl uptake into cells^{3,10} (one component of the cytoplasmic uptake of K^+ discussed above) and in the second case because of extracellular ion depletion resulting from clearance of K^+ by the spatial buffer mechanism.¹¹ The net loss of osmotic particles is, respectively, two times and approximately 1.2 times the flux of K^+ ions out of extracellular space (i.e., the buffer flux f_j in FIG. 1). This factor (2 or 1.2) is denoted by N . If the total tissue osmolarity is Z (ca. 300 mM for mammalian tissue), then the fluid movement into cells to maintain osmotic balance is Nf_j/Z . This fluid is lost from extracellular space, so the K^+ normally present within its volume is transferred to the remaining space at a rate nf_jK_o/Z . The effect on K_o is as if this flux were being added to the remaining space. The resulting (negative) contribution to the buffer capacity due to volume changes ϕ_v is given by:

$$\phi_v = - (n K_o / Z) \phi_j \quad (10)$$

This diminishes the capacity due to the K^+ flux itself (ϕ_j) by only a small fraction, about 2% for KCl uptake and 1.2% for spatial buffering (with $K_o \simeq 3$ mM). The volume changes resulting from KCl uptake and spatial buffering therefore appear to play only a minor role in K^+ buffering compared with the direct effect of the K^+ fluxes. This does not imply, of course, that the quite large changes of extracellular space fraction seen with major K^+ disturbances¹¹ are not important in other ways.

BUFFERING BY FLUID AT A TISSUE SURFACE

A reservoir of fluid at a tissue surface, with relatively stable concentration, tends to buffer K_o near the surface. The fluid acts as a sink for excess K^+ . The concept of a sink capacity σ associated with flux across the surface turns out to be helpful. By analogy with the definition of buffer capacity (Eq. 2), sink capacity σ relates the K^+ flux F_s across the tissue-fluid surface (mol per unit area) to the rate of change of K_o at the surface (dc_o/dt):

$$\sigma = F_s / (dc_o/dt) \quad (11)$$

The sink capacity σ has the dimensions of length. For well-stirred fluid in equilibrium with K_o at the surface, the capacity σ_{stirred} is simply the depth of the surface fluid (FIG. 6). This situation is probably approximated under some conditions by a layer of cerebrospinal fluid bathing brain tissue, several hundred μm thick.

If the fluid at the tissue surface is not well stirred but equilibrates only by diffusion, then the sink capacity $\sigma_{\text{unstirred}}$ depends on the time course of K_o at the surface. High-frequency components affect only the closely adjacent fluid, while low-frequency components influence the K^+ concentration to greater distances and are associated with correspondingly greater sink capacities. Simple diffusion theory shows that $\sigma_{\text{unstirred}}$, for an infinite depth of fluid, is:

$$\sigma_{\text{unstirred}} = (1 - i) (D/4\pi \gamma)^{0.5} \quad (12)$$

This is a vector with a phase lag of 45° and a magnitude about $200 \mu\text{m}$ at 0.01 Hz (FIG. 6B).

The significance of the sink capacity is that it sets a limit to the buffering effects that surface fluid can have on tissue under the surface. σ is the K^+ distribution volume available for buffering at a particular frequency, per unit area of surface. The effective buffer capacity ϕ (i.e., the K^+ distribution space per unit volume of tissue) is graded with depth x below the surface (FIG. 6A), but its total integral ($\int \phi dx$) cannot exceed σ .

Newman^{12,13} has described how the thin layer of neural tissue in the retina (*ca.* $200 \mu\text{m}$ thick) may be buffered by K_o equilibration (via Müller cells) with the surface of the large volume of vitreous fluid within the eye. The present analysis shows that for frequency components around 0.01 Hz , the buffer capacity that could in principle be achieved in this way (if there were full equilibration) would be substantial, averaging 1.0 over the full depth of the retina. The vitreous fluid could never, even under ideal circumstances, buffer very effectively at high frequencies ($\sigma_{\text{unstirred}} \simeq 20 \mu\text{m}$ at 1 Hz), but this may not be important.

The buffer capacities beneath the surface are not easily derived in a general case. They must always be less, however, than in the ideal situation with total constancy of surface K_o ($\sigma = \infty$). With a uniform disturbance q throughout the tissue, and without spatial buffering, there is a characteristic depth ($x \simeq (\alpha D \pi^{-1} \xi^{-1} \gamma^{-1} \lambda^{-2})^{0.5}$) under these conditions at which the buffer capacity has fallen from infinity at the surface to 0.2. In this expression, ξ is the buffer capacity due to the extracellular

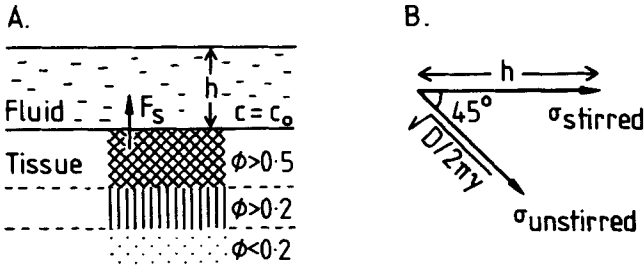


FIGURE 6. Buffering effects due to K^+ exchange with surface fluid. (A) K^+ flux (F_s , per unit area) enters the surface fluid under conditions with a surface concentration displacement c_0 . Buffering in the tissue can be substantial near the surface ($\phi > 0.5$), but declines with depth. (B) The surface sink vector σ ($F_s/(dc_0/dt)$) is shown for well-stirred fluid (depth h) and for deep, unstirred fluid.

space and cells alone ($\xi = \alpha + \phi_c$), assumed for simplicity to be equivalent to a simple distribution space. With $\xi/\alpha = 3$ (cf. FIG. 4), then, this characteristic depth is about $100 \mu\text{m}$ at 0.01 Hz . The effective capacity is 0.5 at about 60% of this depth ($60 \mu\text{m}$). Significant influences due to surface buffering at 0.01 Hz would therefore probably not extend by diffusion alone throughout the whole thickness of the retina ($200 \mu\text{m}$).

TRANSFER OF K^+ BY SPATIAL BUFFERING ACROSS A TISSUE SURFACE

Spatial buffering can improve the degree of equilibration between surface fluid and tissue beneath the surface. It has been proposed that this is an important function of Müller cells in the vertebrate retina^{12,13} and indeed this conclusion is supported by some computer simulations.¹³ A simpler approach is adopted here to estimate the buffer capacity that the Müller cells can achieve and to help to identify some of the critical parameters.

Spatial buffering occurs through a current loop as shown in FIGURE 7. A simplified analysis of this situation¹⁴ treats the buffered interstitial space and the surface fluid as two uniform, discrete compartments. The performance in buffering any one region of tissue by flux to the surface is degraded, by comparison with this model, if the cells have a conductance facing other interstitial compartments. The spatial buffer flux across the surface F_{SB} ($= I/F$ in FIGURE 7, where F is Faraday's constant) is driven by the difference in K^+ equilibrium potential between the two regions of membrane. For small disturbances this driving potential is $RTF^{-1}(c - c_0)/c_B$ where c and c_0 are the disturbances of K_0 at the two sites. The total resistance in the loop for all the cells in unit area of the retina (FIG. 7) is denoted by R_{SB} . F_{SB} is then given by:

$$F_{SB} = RT(c - c_0) (F^2 c_B R_{SB})^{-1} \tag{13}$$

Even if K_o at the retinal surface were absolutely constant ($c_o = 0$), the spatial buffer flux across the surface would be limited in accordance with Equation 13. We can therefore calculate from this equation a maximum sink capacity σ_{SB} ($= F_{SB}/(dc/dt)$) that the Müller cells can utilize in buffering the interstitial compartment:

$$\sigma_{SB} = - iRTF^{-2} (2\pi c_B \gamma R_{SB})^{-1} \tag{14}$$

The corresponding buffer capacity ϕ_{SB} depends on the range of depths, x , through which the buffered interstitial compartment extends:

$$\phi_{SB} = \sigma_{SB} / x \tag{15}$$

This is a vertical vector with a phase lag of 90° , as for other dispersal mechanisms within the tissue (FIG. 5).

For frog retina we can calculate R_{SB} from data cited by Newman.¹³ The input resistance of a single Müller cell is about $18M\Omega$. This appears to be distributed unequally between the endfoot and interstitial zones of the cell membrane, with R_m about $92 M\Omega$ and R_i about $22 M\Omega$ (FIG. 7). About 4,800 Müller cells were estimated per mm^2 . Ignoring the cytoplasmic and extracellular resistances, which are relatively small, this gives R_{SB} about $24 k\Omega mm^2$ ($(92 + 22 M\Omega)/(4,800 mm^{-2})$). With $c_B = 3 mM$, the maximum sink capacity available through spatial buffering ϕ_{SB} (Eq. 14) is $55 \mu m$ at 0.01 Hz. Somewhat more sophisticated calculations, taking account of the limited extent to which diffusion into the vitreous fluid can buffer K_o at the retinal surface (see last section), reduce this estimate by about 20% to $44 \mu m$. The net effect is a buffer capacity (ϕ_{SB} : Eq. 15), distributed throughout the thickness of the retina (ca. 0.2 mm), of about 0.22 at 0.01 Hz. This may be significantly greater than the relatively small extracellular space fraction in the retina ($0.024 - 0.14^{13}$). If cyto-

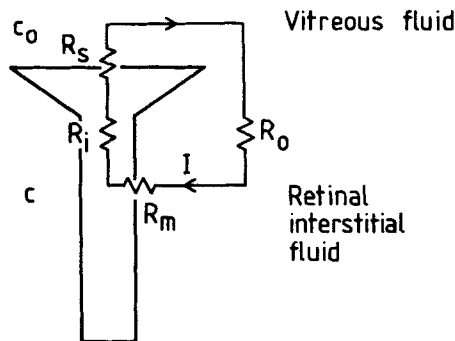


FIGURE 7. Equivalent circuit model for retinal Müller cells. Current I flows in a loop between two fluid compartments: the vitreous fluid with surface concentration displacement c_o and the interstitial (buffered) compartment with concentration displacement c . Resistances are for unit retinal area, lumped in parallel for the individual cells. R_{SB} is the sum of all the resistances in the loop.

plasmic buffering within the retina is similar to that deduced for mammalian brain, however ($|\phi_e|$ ca. 0.5 at 0.01 Hz: FIG. 4), it is not clear that spatial buffering would be important except at rather low frequencies. Newman's calculations to show the benefit of Müller cell action¹³ do not appear to take account of cytoplasmic buffering.

The asymmetric distribution of Müller cell conductance between the regions of membrane facing the endfoot and interstitial space ($R_s < R_m$ in FIG. 7) is a striking feature, which is even more pronounced in the salamander¹² than in the frog. Buffering according to the model of FIG. 7 works best if R_s is made as small as possible. It is therefore good to have as many channels in the endfoot as possible.¹² Brew & Attwell¹⁴ have pointed out, however, that if a fixed number of membrane channels were available per cell, it would be better to distribute them to make $R_s = R_m$ on this model.

Some indication that it may not be appropriate to consider the buffering of the retinal interstitial space as if it were a single compartment is provided by data of Mori *et al.*¹⁵ These results, replotted in FIG. 8, show the distribution of extracellular voltage and potassium changes in the frog retina during spreading depression. This disturbance results in a large K^+ release and an accompanying negative extracellular potential shift lasting about a minute. From the distribution of extracellular potential (FIG. 8A), it is evident that there is a concentration of outward membrane current at the vitreal surface. This was interpreted by Mori *et al.*¹⁵ as current in the Müller cells (FIG. 8B), and indeed provided the first evidence for a specialized conductance of these cells facing the vitreous. In the present context, the interesting feature is that the corresponding inward membrane current within the retina is also highly localized in a zone only about 50 μm deep (25% of the retina), close to the vitreous (FIG. 8B, C). The plots of the distribution of membrane current (FIG. 8C) were calculated on the basis of either a uniform extracellular resistance (hatched) or the markedly non-uniform distribution of extracellular space fraction assumed by Newman¹³ (solid). They both differ markedly from the distribution of the driving force provided by the K^+ increase (FIG. 8D) or the net electrochemical potential of K^+ in extracellular space (FIG. 8D minus).

If the interpretation of these data as attributable to currents in Müller cells is correct,¹⁵ then they suggest that spatial buffer action is much more localized than the distribution of the K^+ increase during spreading depression. This could be explained if there is a concentration of Müller cell conductance not only facing the vitreous fluid, but also facing a zone of interstitial fluid close to the vitreous under these conditions. Such a pattern has not been evident in experiments on isolated Müller cells from the salamander retina.¹² This might be because certain channels in the membrane open only under the extreme conditions of spreading depression,¹⁶ or perhaps because of differences between isolated cells and cells *in vivo*. It would make good sense for buffering action to be concentrated in the neighborhood of structures of the retina that are most critical from this point of view, and for these to be sited close to the vitreal surface. The intrinsically limited sink capacity of the vitreous reservoir could in this site have a concentrated effect both through diffusion and through action of the Müller cells.

According to these ideas, the distribution of Müller cell conductance, possibly modulated significantly by the effects of disturbances such as spreading depression, may be adapted for the different needs of different regions of the retina. The low-conductance zone in the bulk of the retina, farthest from the vitreous, makes a relatively small contribution to the buffering of the higher-frequency components of a disturbance, even around 0.01 Hz as discussed above. It nevertheless contributes a substantial buffering capacity for disturbances with lower-frequency components, which may be important in the retina with slowly changing light levels.

THE ROLE OF GLIAL COUPLING IN SPATIAL BUFFERING

The roles of gap junctions and of electrical coupling between glial cells have been rather little studied. Coupling means that, in principle, glial cells may form a syncytium, which permits spatial buffer currents to flow farther than the dimensions of a single cell.² This makes little difference, however, if glial cells have processes that are much longer than their own space constant, which may be the case in vertebrate brain, since adjacent regions of overlapping cells are then almost isopotential.²

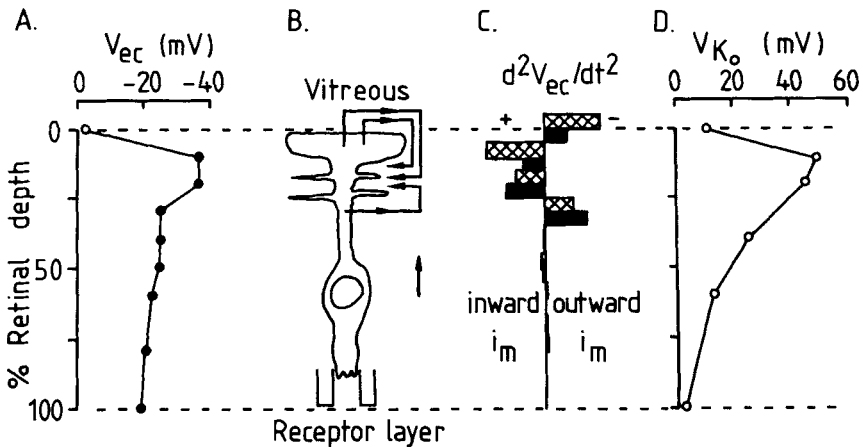


FIGURE 8. Current associated with spreading depression (SD) in frog retina. Replotted and calculated from Mori *et al.*,¹⁵ Figures 1(o) and 2(•). (A) Peak extracellular voltage changes (V_{ec}) during SD elicited by a light flash. (B) Current loops in Müller cells, inferred from (A). (C) Current source density (arbitrary units) inferred from A, assuming (1) uniform extracellular resistance (hatched, equal to d^2V_{ec}/dt^2) and (2) resistivity proportional to α^{-1} at different depths, according to Newman¹³ (solid). (D) Potential shift from an extracellular K^+ electrode (V_{K_o}) measuring K_o increases during SD, 9 seconds after the flashes (approximately the time of measurement of the voltage changes in A). Currents attributed to spatial buffering (B,C) are more localized than the increase of K^+ chemical potential (D).

Not enough is known to assess the role of astrocyte coupling in vertebrate brain. Data for coupling between Müller cells in the axolotl retina has, however, been obtained recently by Attwell *et al.*,¹⁷ and it has been suggested by the authors that this coupling may play a significant role in K^+ buffering. We can use these data and the present analysis to estimate the buffer parameters. Direct observations showed that membrane potential changes in one cell were attenuated to about 10% in the nearest neighbors 25–30 μm apart.¹⁷ The network was modeled by the authors as a square two-dimensional lattice of cells (FIG. 9) at a spacing of 30 μm , each with a membrane resistance of 16 $\text{M}\Omega$ and with coupling to each immediate neighbor through 160 $\text{M}\Omega$ junctions. The lateral space constant for the network (Λ in Eq. 9) was about 12 μm .

Even if the coupling ratio for glial cells is substantial, this does not necessarily imply significant buffering action unless the cell and junction resistances are themselves low. The factor by which diffusion is enhanced through lateral spatial buffer action depends, according to Equations 8 and 9, on the ratio of the intracellular (in this case, chiefly junctional) resistance and the extracellular resistance. The extracellular resistance corresponding to the coupling resistance between the Müller cells ($R_j = 160 \text{ M}\Omega$) is that between two opposite sides of the $30 \mu\text{m}$ lattice (a,b, in FIG. 9). Assuming extracellular parameters $\alpha = 0.1^{13}$ and $\lambda^2 = 2.5$ as for rat cortex^{1,2} and an extracellular resistivity $1 \Omega\text{m}$, r_o is $120 \text{ k}\Omega$ for the 0.2-mm thickness of the retina. Substituting in Equation 8 gives $\beta = 0.066$, which corresponds to an increase of the diffusion flux due to spatial buffering (Eq. 9) of 3.3-6.6% for wavelengths greater than $75 \mu\text{m}$. It is difficult to see how such spatial buffer action can be quantitatively

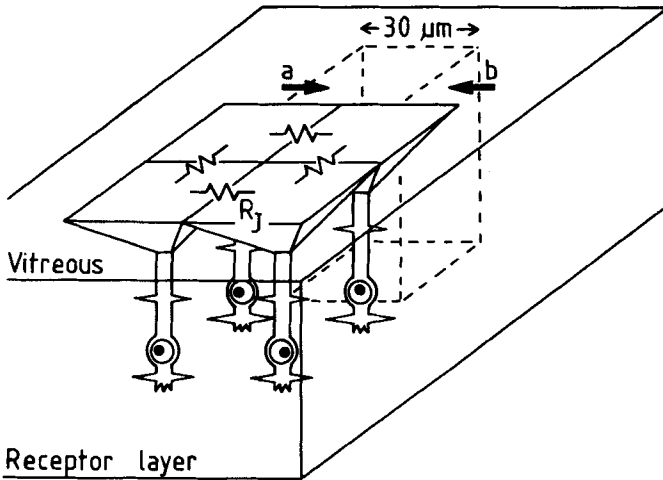


FIGURE 9. Coupling between Müller cells in axolotl retina. The network used by Attwell *et al.*¹⁷ to fit their data: a square array of Müller cells with $30 \mu\text{m}$ spacing. Junctional resistances $R_j = 160 \text{ M}\Omega$ may comprise junctions at any depth; a and b indicate a block of tissue for which extracellular resistance is calculated.

very significant for lateral dispersal in the axolotl retina, unless the junctional resistances are substantially less under critical buffering circumstances than those measured. This leaves wide open the question what, if anything, may be the physiological role of coupling between Müller cells.

SUMMARY

A new concept, that of "buffer capacity," is defined for potassium-buffering mechanisms in neural tissue. Buffer capacities for different mechanisms can be added and compared, thus simplifying quantitative assessment of diffusion, cytoplasmic uptake,

and spatial buffering under varied conditions. The characteristic frequency components for potassium disturbances due to neural events are identified. The effect of buffering by a reservoir of fluid at a tissue surface is analyzed, together with its intrinsic limitations. The role of retinal Müller cells in spatial buffering is considered quantitatively: both buffering to the tissue surface and buffering sideways through cell-to-cell connections.

ACKNOWLEDGMENT

I am grateful to David Attwell, Charles Nicholson, and Anne Warner for helpful comments on a draft manuscript.

REFERENCES

1. NICHOLSON, C. & J. M. PHILLIPS. 1981. Ion diffusion modified by tortuosity and volume fraction in the extracellular microenvironment of the rat cerebellum. *J. Physiol. London* **321**: 225-257.
2. GARDNER-MEDWIN, A. R. 1983. Analysis of potassium dynamics in brain tissue. *J. Physiol. London* **335**: 393-426.
3. GARDNER-MEDWIN, A. R. 1980. Membrane transport and solute migration affecting the brain cell microenvironment. *Neurosci. Res. Prog. Bull.* **18**: 208-226.
4. GARDNER-MEDWIN, A. R. 1981. Possible roles of vertebrate neuroglia in potassium dynamics, spreading depression, and migraine. *J. Exp. Biol.* **95**: 111-127.
5. GARDNER-MEDWIN, A. R. 1983. A study of the mechanisms by which potassium moves through brain tissue in the rat. *J. Physiol. London* **335**: 353-374.
6. GARDNER-MEDWIN, A. R. & C. NICHOLSON. 1983. Changes of extracellular potassium activity produced by electric current through brain tissue in the rat. *J. Physiol. London* **335**: 375-392.
7. ORKAND, R. K., J. G. NICHOLLS & S. W. KUFFLER. 1966. Effect of nerve impulses on the membrane potential of glial cells in the central nervous system of amphibia. *J. Neurophysiol.* **29**: 788-806.
8. GARDNER-MEDWIN, A. R. 1985. The space constant for glial potassium buffering in the isolated frog brain. *J. Physiol. London* **365**: 52P.
9. GARDNER-MEDWIN, A. R. 1985. Assessment of the glial "spatial buffer" mechanism in rat brain, frog brain, and retina. *In* Functions of Neuroglia. A. I. Roitbak, Ed. Sov. Acad. Sci. In press.
10. BOYLE, P. J. & E. J. CONWAY. 1941. Potassium accumulation in muscle and associated changes. *J. Physiol. London* **100**: 1-63.
11. DIETZEL, I., U. HEINEMANN, G. HOFMEIER & H. D. LUX. 1980. Transient changes in the size of the extracellular space in the sensorimotor cortex of cats in relation to stimulus-induced changes in potassium concentration. *Exp. Brain Res.* **40**: 432-439.
12. NEWMAN, E. A. 1984. Regional specialization of retinal glial cell membrane. *Nature London* **309**: 155-157.
13. NEWMAN, E. A., D. A. FRAMBACH & L. L. ODETTE. 1985. Control of extracellular potassium levels by retinal glial cell siphoning. *Science* **225**: 1174-1175.
14. BREW, H. & D. ATTWELL. 1985. Is the potassium-channel distribution in glial cells optimal for spatial buffering of potassium? *Biophys. J.* **48**: 843-847.
15. MORI, S., W. H. MILLER & T. TOMITA. 1976. Müller cell function during spreading depression in frog retina. *Proc. Natl. Acad. Sci. USA* **73**: 1351-1354.

16. GARDNER-MEDWIN, A. R. 1985. Potential challenge from glia. *Nature* **315**: 181.
 17. ATTWELL, D., H. BREW & P. MOBBS. 1985. Electrophysiology of the Müller cell network in the axolotl retina. *J. Physiol. London Proc.* **369**: 33P.
-

DISCUSSION

J. ZADUNAISKY (*New York University Medical Center, New York, NY*): If there is so much potassium-buffering capacity, why is there edema sometimes?

A. R. GARDNER-MEDWIN (*University College London, London, England*): The volume changes are very small when the potassium disturbances are small and such volume changes don't account for very significant effects on the potassium buffering, which is what I have been discussing. Edema presumably only develops in extreme circumstances.

E. A. NEWMAN (*Eye Research Institute of Retina Foundation, Boston, MA*): I agree with you that my original estimates of the membrane conductance of the cell were probably underestimates so that the buffer capacity of Müller cells may be larger. My data suggest, however, that the membrane of the Müller cells in the outer plexiform layer is specialized. I'd like to point out that I don't think you can use data from Mori *et al.* (*Proc. Natl. Acad. Sci.* **73**: 1351-1354, 1976) as evidence for a high conductance in the inner plexiform layer, because it is very difficult to get a true idea of this distribution of potassium increase by radial penetrations of the tissue with microelectrodes.

GARDNER-MEDWIN: It would be good to have further studies of the retina during spreading depression, but I don't see any obvious alternative explanation for the data of Mori *et al.* (1976).

NEWMAN: I'd like to make another comment. I'm not sure if your model for assessing buffering by Müller cells was based on an unstirred layer, but as we saw in brain siphoning, the capacity to move potassium to CSF and the blood vessels is increased because both these fluids are moving.

GARDNER-MEDWIN: My estimates for the Müller cell buffering are about 20% smaller without stirring than with stirring (at 0.01 Hz). The influence of stirring in the vitreous would be greater if the Müller cells had higher conductances.

E. M. WRIGHT (*University of California, Los Angeles, CA*): There is a ciliated surface in the ventricle. The cilia are moving at 20 cycles a second out to a distance of 200 micrometers. I don't know about in the eye, but in the ventricular fluid in the brain it's usual for cilia to stir at five times their length. We measured this in the frog brain and measured the rate of efflux from the parenchyma into the CSF. We turned the cilia on and off, and we could change the effective diffusion constant for ions coming out of the brain.

GARDNER-MEDWIN: I am sure this could be important.

T. H. MAREN (*University of Florida College of Medicine, Gainesville, FL*): How are you using the term buffer here?

GARDNER-MEDWIN: What I mean by a buffer is a mechanism that reduces the concentration changes below the level that they would be if that mechanism were not present.